*Journal of*
*Nanoscience and Nanotechnology*
Vol. 7, 1–7, 2007

# Extraction of Chlorpyrifos and Malathion from Water by Metal Nanoparticles

A. Sreekumaran Nair and T. Pradeep*

*DST Unit of Nanoscience, Department of Chemistry and Sophisticated Analytical Instrument Facility, Indian Institute of Technology Madras, Chennai 600036, India*

The nanoparticles of gold and silver in solution state and supported over activated alumina are effective systems for the quantitative removal of chlorpyrifos and malathion, two common pesticides found in surface waters of developing nations, from water. In the solution phase, these pesticides adsorb onto the nanoparticles' surfaces and upon interaction for a long time, the nanoparticles with adsorbed pesticides precipitate. In contrast, complete removal of these pesticides occurs when contaminated water is passed over nanoparticles supported on alumina. A prototype of an on-line filter was made using a column of activated alumina powder loaded with silver nanoparticles and the device was used for pesticide removal for extended periods. We believe that the method has great technological potential in drinking water purification, especially using silver nanoparticles.

**Keywords:**

RESEARCH ARTICLE

## 1. INTRODUCTION

Synthetic organic chemicals account for nearly one-third of the chemical production in industrialized countries and many of these find their way into the environment.[1] Chlorinated solvents are the most prevalent contaminants, besides chlorine containing pesticides.[2] Many of these chemicals pose imminent threat to the inhabitants of earth.[3–7] The financial burden involved in the cleanup of these contaminated soils and/or water is colossal. As a result, researchers turned to nanotechnology for an efficient, economic, and eco-friendly method to rectify this problem.[8–11] The use of metal nanoparticles for environmental remediation is a relatively new area of research in which only limited progress has happened so far.[8–11] Nanoscale particles are promising in this area because of their unique properties such as small particle sizes, large surface to volume ratio[12, 13] and the ease with which they can be anchored onto the solid matrices for enhanced treatment of water, waste water, and gaseous process streams. The use of nanoscale iron particles for environmental remediation is a recent advance in this area.[8–11] Both bare as well as palladized iron nanoparticles was used for degrading a wide variety of halogenated organic compounds (both aliphatic and aromatic). Nanoscale Fe powders were also used in degrading two most common pesticides in water, namely DDT, and lindane.[8] The use of metal nanoparticles of silver and gold in the degradation of a variety of halocarbons was reported recently.[14, 15] We have also shown that nanoparticles can be used in the detection and extraction endosulfan, a pesticide with acute toxicity and long persistence in human body.[16]

Chlorpyrifos, *O*,*O*-Diethyl-*O*-(3,5,6-trichloro-2-pyridyl) phosphorothioate ($C_9H_{11}Cl_3NO_3PS$), an organophosphate insecticide, is one of the most-widely used active ingredients for pest control products worldwide.[17, 18] Like other organophosphates, its insecticidal action is due to the inhibition of the enzyme acetylcholinesterase, resulting in the accumulation of the neurotransmitter, acetylcholine, at nerve endings.[19] This results in excessive transmission of nerve impulses, which causes mortality in the target.[19] It is a degradable molecule and breaks down in the environment when exposed to microorganisms, chemical reactions, and sunlight.[20] Malathion, *S*-1,2-bis(ethoxycarbonyl) ethyl *O*,*O*-dimethyl phosphorodithioate, is suspected to cause child leukemia, anemia, kidney failure, and human birth defects, is another widely used pesticide in developing countries.[21, 22] It is believed to be an agent in causing DNA abnormalities at all doses.[23, 24] There were reports of malathion causing "deletions" in one section of the chromosome thereby inducing mutations in human beings.[25–27] Malathion can persist in the human body for at least two generations.[28, 29] In this paper we describe the complete removal of the two pesticides, chlorpyrifos and malathion with silver and gold nanoparticles loaded on alumina, a methodology which has been

*Author to whom correspondence should be addressed.

implemented in the laboratory for water purification. These two pesticides are the most common ones preset in the surface waters of India; the other two being lindane and DDT. The construction of an on-line filter is cost effective, especially with silver, as the particles are in the nano form.

## 2. EXPERIMENTAL DETAILS

Technical grade (99.5%) chlorpyrifos and malathion were obtained from CHEM SERVICE, Inc., USA, and used as received. Chloroauric acid ($HAuCl_4 \cdot 3H_2O$) and $AgNO_3$ were from CDH and Qualigens fine chemicals, India, respectively. Activated alumina globules were from local sources and used as received. Activated alumina powder (neutral, Brockmann grade 1 for chromatographic analysis, particle size (mesh) ~150) was from CDH, India. Trisodium citrate was from SRL, India and used as received. Nanopure water obtained by further purification of triply distilled water by UHQ ultra water purifier of ELGA was used for all the synthesis and measurements. The syntheses of Au@citrate and Ag@citrate (the terminology implies that citrate ions cover the nanoparticle surface in solution) were done according to the literature procedures.[30, 31] Briefly, the synthesis involves the following materials and methods: 200 ml (8 ml in the case of gold) of 0.005 M stock solution of silver nitrate ($HAuCl_4 \cdot 3H_2O$ for gold) in water was diluted to 1 l (152 ml for Au) and heated until it begins to boil. 40 ml of 1% sodium citrate solution (8 ml 0.5% for Au) was added and heating continued till the color was pale yellow (pink for Au). The average particle size was 10–20 nm for Au,[30] and 60–80 nm for Ag.[31] The as prepared solutions were used for conducting solution phase experiments. Supported nanoparticles were prepared by the following method. To 1 l of the as prepared solution of Ag@citrate or Au@citrate in hot condition, half a kg of alumina globules (average diameter 0.5 cm) were soaked and kept for a minimum period of 6 h to ensure saturable adsorption of nanoparticles on the alumina surface (checked by taking the absorbance of nanoparticle solution at periodic intervals. After 6 h, there was no decrease in the absorbance of nanoparticle solution indicating their saturable adsorption on the oxide surface). The intake of nanoparticles per alumina globule is high (~0.116 mg per globule on an average, however this depends on its size as well). The alumina globules were washed several times with distilled water and air-dried. These materials will be described as $Al_2O_3$@Ag and $Al_2O_3$@Au in the subsequent discussions. We studied the interaction of 10, 5, 2, 1, and 0.1 ppm aqueous solutions of chlorpyrifos and malathion with both bare (Au@citrate and Ag@citrate, in solution phase) as well as supported nanoparticles using UV-Visible spectroscopy. The adsorption of pesticides on nanoparticles is manifested in the gradual decrease in absorbance of the pesticide with time. In a typical procedure, 10 ml aqueous solution of chlorpyrifos or malathion in required concentration (ppm) was treated with 15 (an arbitrary number) globules of $Al_2O_3$@Ag (or $Al_2O_3$@Au) and the progress of adsorption of pesticide on the nanoparticles' surfaces was monitored from the absorption spectra of the solution at periodic intervals (20 minutes). 3 ml aliquots of the solution were taken out for analysis by UV-Visible spectroscopy and the solutions were put back after the measurements. The solution was occasionally shaken for better contact between the surfaces of nanoparticles and the pesticide solution. The complete removal of the pesticide from water occurs by this method though it is a time-dependent process. However, the removal was achieved quickly using the nanoparticles loaded on activated alumina powder. This was done so as to demonstrate the use of a practical on-line filter. 250 g of activated alumina powder was filled in a glass column of 50 cm length and 3 cm diameter with a silica frit at the bottom. The silver or gold nanoparticle solution prepared as above was poured from the top of the column. The solution came out was colorless indicating the complete adsorption of nanoparticles on alumina surfaces. 6 l of the as-prepared nanoparticle solution were required for saturable loading on the alumina surfaces (corresponding to 259.2 mg Ag/100 g of alumina, mesh ~150). After saturable adsorption, the alumina surface became golden yellow/pink depending on whether silver/gold was loaded. Subsequent pouring of the nanoparticle solution does not lead to adsorption on alumina. The column was washed with distilled water thrice to remove the adsorbed metal ions or citrate used for synthesis. 50 ppb chlorpyrifos solution was made by dissolving 0.5 mg of it in 10 l of distilled water. 1 l of the above solution was taken as blank and the chlorpyrifos in it was extracted thrice with 150 ml of *n*-hexane. This was then concentrated to ~2 ml in a rotavapor (maintained at 40 °C) and was made up to 10 ml in a standard flask using hexane. The amount of pesticide in the solution was quantitated using UV-Visible spectroscopy and gas chromatography (GC). The remaining pesticide solution was passed through the column and 1 l each of the solution was collected at regular intervals and the pesticide content was analyzed as above by UV-Visible spectroscopy and GC. For IR and Raman measurements, the liquid phase reaction was carried out in bulk in closed vessels and the residue was collected by centrifugation. The as-synthesized nanoparticles were characterized by UV-Visible spectroscopy and transmission electron microscopy (TEM). The TEM images were taken with a Philips CM12 microscope working under 120 keV acceleration. The UV-Visible spectra were recorded with a Perkin Elmer Lambda 25 spectrometer. The infrared spectra were taken with a Perkin Elmer Spectrum One spectrometer. The samples were prepared in the form of 1% (by weight) KBr pellets and all the spectra were measured with a resolution of 4 $cm^{-1}$. The IR spectrum of malathion (a liquid) was taken using a liquid cell. Raman analyses (of the dried residue as detailed below) were performed with a Bruker IFS 66 v FT Raman spectrometer.

The gas chromatography measurements were done using an instrument from Mayura Analytical Pvt. Ltd., India, fitted with a pulse discharge electron capture detector.

## 3. RESULTS AND DISCUSSION

Figure 1 shows the changes in the optical absorption spectrum of Au@citrate upon exposure to 2 ppm chlorpyrifos. Trace a is the absorption spectrum of Au@citrate having an absorption maximum of 522 nm (2 ml taken in the UV-Visible cuvette after diluting with equal volume of water) and b was taken immediately after the addition of 2 ml of 2 ppm chlorpyrifos to 2 ml of the nanoparticle solution. The subsequent traces (c–r) were taken at 20 minutes intervals of time. As can be seen from the spectra, the plasmon absorption of Au at 522 nm decreased in intensity and another broad plasmon emerged at longer wavelength, after 40 minutes. The intensity of the plasmon at longer wavelength increased with time, accompanied by further red shift. The dampening of the intensity of the original plasmon and the emergence of a broad absorption feature at longer wavelengths are due to the adsorption of chlorpyrifos on the nanoparticles' surfaces, followed by the particle aggregation through interlocking.[16, 32, 33] At this stage the solution turned pale-blue and the pesticide-adsorbed nanoparticles began to precipitate. Centrifugation of the solution resulted in complete precipitation of the material. An identical reaction sequence was noticed with Ag nanoparticles also, but the red shift in plasmon excitation was not well pronounced as in the case of Au. This is because the change in the dielectric constant of silver upon pesticide binding is less compared to that of gold.[16]

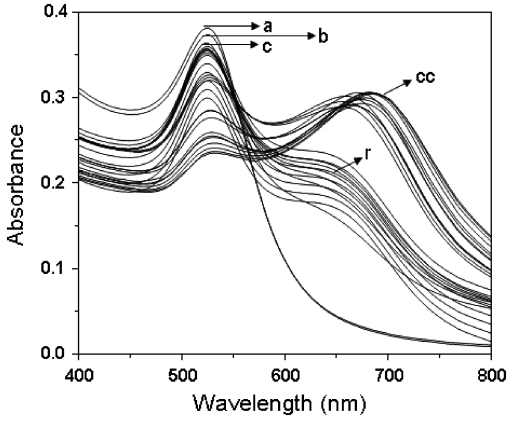


**Fig. 1.** Time dependent UV-Visible spectra showing the adsorption of chlorpyrifos on Au nanoparticles. Trace a is the absorption spectrum of 2 ml of Au@citrate (after diluting with equal volume of water) showing the absorption maximum at 522 nm. Traces b was taken 20 minutes after the mixing of 2 ml of 2 ppm chlorphrifos (in water) with it. After 40 minutes, the plasmon excitation absorption at 522 nm decreases in intensity and another broad absorption feature emerges at longer wavelength (trace c). At this stage the solution turns pale blue in color. This can be attributed to the beginning of adsorption of chlorpyrifos on Au nanoparticles surface and their subsequent aggregation through interlocking. With further passage of time, the plasmon absorption at 522 nm decreases in intensity and that at longer wavelength gains in intensity accompanied by further red shift. This is due to the time dependent adsorption of chlorpyrifos on the nanoparticles' surfaces. Subsequent traces were recorded at 20 minutes intervals thereafter. After 4 hours (trace cc), the completely blue particles begin to precipitate through aggregation.

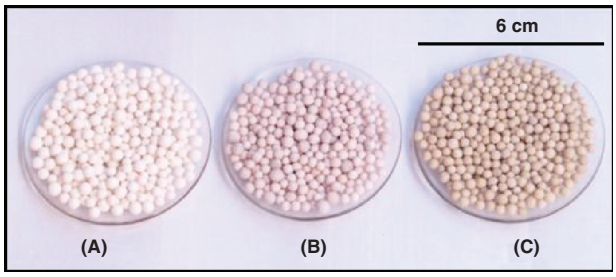


**Fig. 2.** Photographs of pure alumina (A) and alumina samples after coating with nanoparticles of gold (B) and silver (C). The white alumina surface becomes brilliantly colored as a result of nanoparticle incorporation.

Having found that the pesticides adsorb on the nanoparticles' surfaces, we used supported nanoparticles of Au and Ag for their quantitative removal from water. Figure 2 shows the photographs of pure alumina (A) and Au and Ag nanoparticles supported on alumina, respectively (B and C). Due to the incorporation of the nanoparticles, the white surface of alumina became brilliantly colored (yellow in the case of silver and pale pink in the case of gold). The air-dried globules were used for the quantitative removal of pesticides from water. The nanoparticle-coated materials are stable in air for several months in the laboratory atmosphere.

Figure 3 shows time dependent UV-Visible spectra of 1 ppm solution of chlorpyrifos exposed to $Al_2O_3$@Ag, showing its complete removal from water. A 3 ml aliquot of the solution was taken out every time for the UV-Visible measurements (which was put back after the measurements to simulate the same experimental conditions throughout the process). In Figure 3, trace a is the absorption spectrum of 1 ppm chlorpyrifos having an absorbance of 0.147 and $\lambda_{max}$ at 267 nm (Ref. [34]) (in acetonitrile-methanol mixture chlorpyrifos shows three peaks at 202, 230, and 289 nm, respectively, in the wavelength window of 200–350 nm. However, in water we have seen only one peak at 267 nm, possibly due to merging of the latter two peaks). Trace b was recorded 20 minutes after soaking 15 globules of $Al_2O_3$@Ag into 10 ml of the pesticide solution. There was a small increase in the background of the subsequent traces and a small hump came-up at 350 nm, possibly due to the leaching of a small amount of particulate matter when $Al_2O_3$@Ag is soaked into the solution. Subsequent traces (c–r) were taken at intervals of 20 minutes. The reduction in absorbance of chlorpyrifos at 266 nm was abrupt at the initial stages but subsequently became continuous corresponding to the kinetics of adsorption. Trace s is the absorption spectrum of the solution taken after 10 h showing the complete

RESEARCH ARTICLE

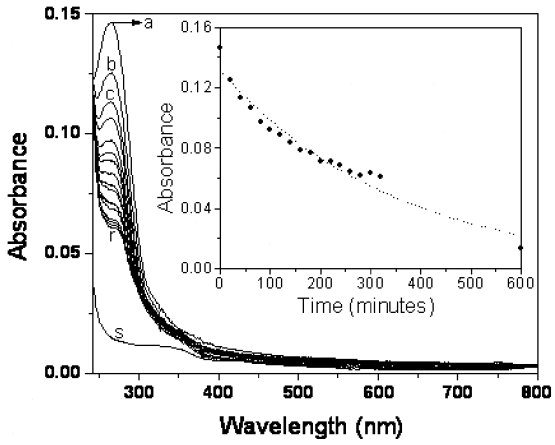


**Fig. 3.** The time dependent UV-Visible spectra showing the adsorption of 1 ppm chlorpyrifos on $Al_2O_3$@Ag. Trace a is the absorption spectrum of 1 ppm chlorpyrifos and b is the absorption spectrum of the solution, 20 minutes after soaking the supported nanoparticles in the pesticide solution. The subsequent traces (c–r) were taken at 20 minutes intervals thereafter. Small increase in background and a minor hump are also visible in the traces (c–r), possibly due to the formation of small quantities of Ag+ in solution. Trace s was taken after 10 hours showing the complete disappearance of chlorpyrifos from water. The inset shoes decrease in absorbance versus time from the absorption spectroscopy data for the traces (a-s). The dotted line in the inset shows a fit of the exponential decrease in absorbance with time.

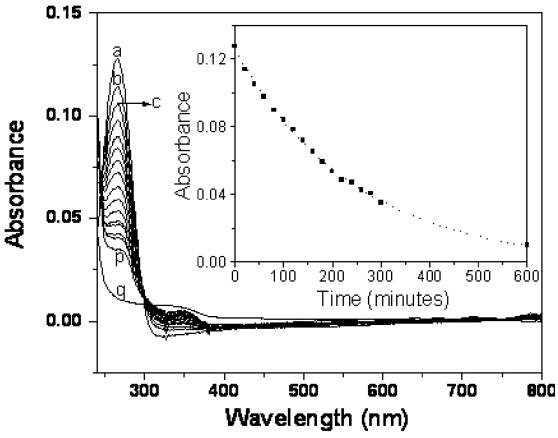


**Fig. 4.** The time depedent UV-Visible spectrum showing the adsorption of 1 ppm malathion on $Al_2O_3$@Ag. Trace a is the absorption spectrum of 1 ppm malathion having an absorption maximum at 267 nm and b is that of the solution taken 20 minutes after soaking the supported nanoparticles in the pesticide solution. The subsequent traces (c–p) were taken at 20 minutes intervals thereafter. Trace q was taken after 10 hours showing the complete disappearance of malathion from water. The inset shows the decrease in absorbance versus time for the reaction for the traces (a–q). The dotted line in the inset shows a fit of the exponential decrease in absorbance with time.

disappearance of chlorpyrifos from water. A minor hump is seen at around 350 nm in this case also. The decrease in absorbance of the pesticide versus time is shown in the inset. The dotted line in the inset shows a fit of the exponential decrease in absorbance with time. Similar reaction sequences were noticed in the reaction of 2 ppm chlorpyrifos too.

Figure 4 represents the UV-Visible spectra showing the adsorption of 1 ppm malathion on $Al_2O_3$@Ag in a time-dependent manner. In Figure 4, trace a is the absorption spectrum of 1 ppm malathion and b was taken 20 minutes after soaking $Al_2O_3$@Ag in the malathion solution. Subsequent traces (c–p) were taken at intervals of 20 minutes. The progressive reduction in the absorbance of the UV feature of malathion is due to its adsorption on the nanoparticles' surfaces. Trace q was taken after 10 h showing the complete disappearance of malathion from water. The minor hump seen at 350 nm could be due to the leaching of a small amount of the particulate matter from alumina into the solution. The inset of Figure 4 shows the plot of decrease in the absorbance versus time for the traces (a–q). The dotted line in the inset shows a fit of the exponential decrease of absorbance with time. Similar reaction profiles were noticed in the case of 2 ppm malathion with $Al_2O_3$@Ag and $Al_2O_3$@Au, respectively.

Figure 5 shows the time dependent UV-Visible spectra of the reaction between 2.5 ppm malathion and $Al_2O_3$@Au. Trace a is the absorption spectrum of malathion and trace b was taken 20 minutes after soaking $Al_2O_3$@Au globules into the pesticide solution. Subsequent traces (c–p) were taken at 20 minutes intervals thereafter. Complete removal of malathion from water took place after 10 h of treatment with the supported nanoparticles, as is evident from the last trace (trace q).

Figure 6(A) shows the infrared spectrum of chlorpyrifos (a) and that adsorbed on Ag nanoparticles' surface (b). In the spectrum a, the IR features of chlorpyrifos are seen at 738, 835, 1018, 1170, 1414, 1548 $cm^{-1}$ respectively.[35, 36] The doublet at 2986 $cm^{-1}$ shows the features of symmetric and antisymmetric stretching of the methylene groups.

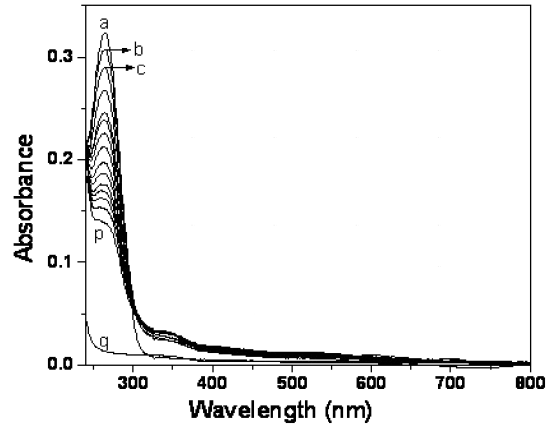


**Fig. 5.** The time depedent UV-Visible spectra of the reaction between 2.5 ppm malathion and $Al_2O_3$@Au. Trace a is the absorption spectrum of 2.5 ppm malathion. Trace b was taken 20 minutes after soaking the globules into the pesticide solution. Subsequent traces (c–p) were recorded at 20 minutes intervals. The gradual decrease in the absorbance of solution is due to the adsorption of malathion on the nanoparticles' surface. Trace q was taken after 10 hours showing the complete disappearance of malathion from water.

RESEARCH ARTICLE

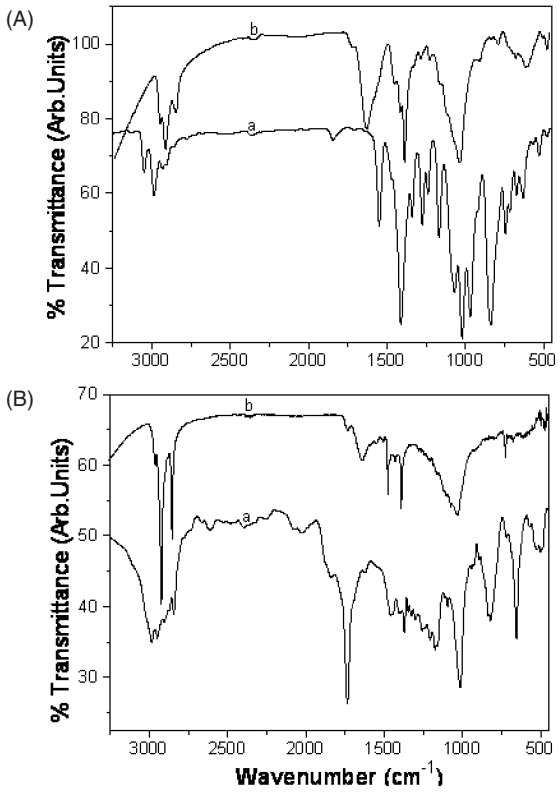


**Fig. 6.** The IR spectra of pure pesticides and those a adsorbed on the nanoparticles's surface. In Figure A, trace a is the IR spectrum of chlorpyrifos and b, that adsorbed on Ag nanoparticles' surface. All the IR features of chlorpyrifos are broadened and shifted from their parent positions because of adsorption on the surface of nanoparticles. there is also large change in intensities. Figure 6(B) shows the IR spectra of pure malathion (a) and that adsorbed on Ag surface (b). The shift and broadening of the infrared features of the pesticide due to adsorption on the nanoparticles' surface are clearly visible from the trace. The additional peaks observed are due to the citrate impurity.

In trace b (the IR spectrum of chlorpyrifos adsorbed on Ag nanoparticles' surfaces), almost all the features of chlorpyrifos were broadened, accompanied with substantial shifts confirming the binding of chlorpyrifos on the nanoparticles' surfaces. Variation in the intensities of the peaks could be attributed to changes in the symmetry of the vibrations upon adsorption. We believe that the sulphur and halogen atoms in the chlorpyrifos interact strongly with the nanoparticles' surfaces resulting in the adsorption of the pesticide. There are substantial shifts for $\nu$P=S (at 1548 cm$^{-1}$) and $\nu$C–Cl (at 738 cm$^{-1}$) of the chlorpyrifos (trace a) upon adsorption onto the nanoparticles' surfaces (trace b). Similarly Figure 6(B) shows the IR spectra of the malathion (a) and the malathion adsorbed on Ag nanoparticles' surfaces (b). In this case also, the infrared features of malathion were broadened and shifted because of its close proximity to the nanoparticles' surfaces. Similar observations were noticed in Raman spectroscopic measurements also, though with reduced intensities.

In order to confirm that the pesticides are indeed adsorbed on nanoparticles' surfaces, a control experiment

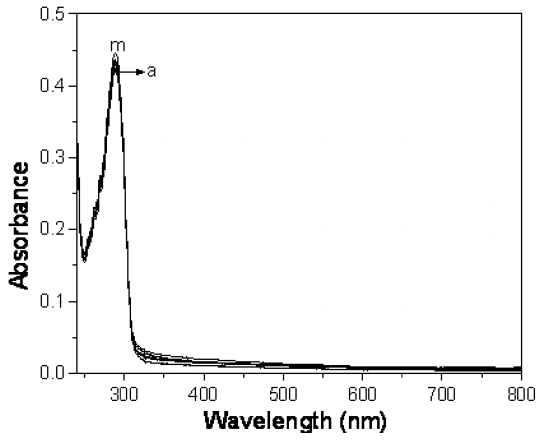


**Fig. 7.** The time dependent UV-Visible spectra showing the interaction of pure $AL_2O_3$ and chlorpyrifos. Trace a is the absorption spectrum of 3 ppm chlorpyrifos. subsequent traces were taken at 20 minutes intervals after treating with pure $Al_2O_3$. The adsorbance of chlorpyrifos doesn't decrease with time implying that pure alumina alone cannot adsorb the pesticide. There is a small increase in the background of the traces because of the leaching of particulate matter into solution.

was performed by treating pure $Al_2O_3$ with chlorpyrifos solution under the same experimental conditions. Figure 7 shows the time dependent UV-Visible spectra showing the effect of exposure of a 3 ppm chlorpyrifos solution to pure $Al_2O_3$. Trace a is the absorption spectrum of 3 ppm chlorpyrifos. The subsequent traces (up to m) were recorded at 20 minutes intervals. There was an increase in the background of the subsequent traces, after the addition of $Al_2O_3$ globules, due to the leaching of small amount of alumina particles into the solution (thereby contributing to scattering). There was no decrease in the intensity of the absorption feature of chlorpyrifos, implying the inability of activated $Al_2O_3$ alone to remove it. The same was verified in the case of malathion also.

While the above experiments resulted in complete removal of the pesticides from water in a time-dependent manner, we thought it is important to demonstrate the removal of pesticides at concentrations relevant to the environment. We thought it is worthwhile to explore the use of this technology for drinking water purification, especially in rural areas of India where pesticide contamination is an important issue. An on-line device was made as described in the experimental section using 250 g of activated alumina powder impregnated with Ag nanoparticles. 10 l of 50 ppb chlorpyrifos solution was used as input water for experiments, much above the concentrations found in surface waters. 1 l of the above solution was taken as blank and the chlorpyrifos in it was extracted thrice with 150 ml aliquots of *n*-hexane. The total extract was concentrated to ~2 ml in a rotavapor and was made upto 10 ml in a standard flask using hexane. Trace a in Figure 8 represents the absorption spectrum of this solution showing the chlorpyrifos peak at 292 nm. The remaining pesticide solution (9 l) was passed through the column and 1 l each of the solution was collected at varying time intervals.

RESEARCH ARTICLE

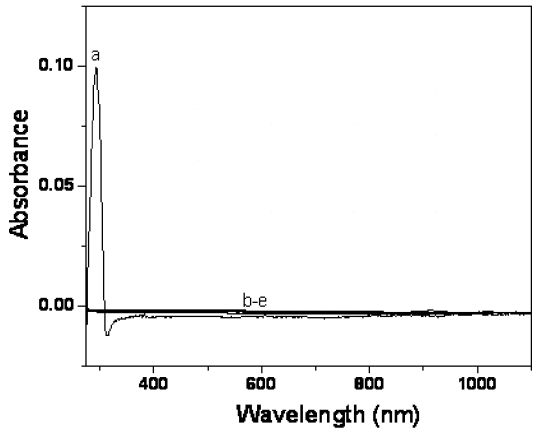


**Fig. 8.** Set of UV-Visible spectra showing the complete disappearance of chlorpyrifos from water when passed through a column of alumina loaded with nanoparticles. Trace a is the absorptioon spectrum of chlorpyrifos extracted from water with hexane, concentrated and made-up to 10 ml and (b–e) are the absorption spectra of the extract made under similar procedure after the pesticide containing water was passed through the column. Note that in the hexane extracts (b–e), the absorption feature of chlorpyrifos has disappeared, implying its complete removal from water.

This was done to check the effectiveness of the device for extended use and the pesticide content was analyzed as above. Traces (b–e) represent the UV-Visible spectra of the hexane extract (concentrated and made up to 10 ml with hexane) collected at 4 different intervals (e being the last 1 l flown through the column), showing the complete disappearance of chlorpyrifos from water. Similar results were obtained with malathion too.

The complete removal of chlorpyrifos from water was also confirmed by gas chromatographic analysis. Figure 9 shows the gas chromatogram of the samples (a–e) mentioned above. Figure 9(A) shows the chromatogram of the blank solution (a) (details mentioned above). The peak at 2.140 min is due to the solvent (hexane) and that at 2.933 min is due to the chlorpyrifos. Figure 9(B) shows the chromatogram of the sample b mentioned above (obtained after passing the chlorpyrifos solution through the activated alumina loaded with nanoparticles) showing the complete removal of chlorpyrifos from water. Similar results were obtained for samples (c–e) also. Experiments with malathion also gave similar results. This on-line device was used for pesticide removal for over three months with little reduction in its efficiency. We have also performed the pesticide removal experiments with natural water instead of triply distilled water and found that device works with comparable efficiency.

## 4. CONCLUSIONS

Both bare nanoparticles and those supported on alumina are excellent systems for the removal of the common pesticides, chlorpyrifos, and malathion from water. The time dependent removal of these pesticides from water was

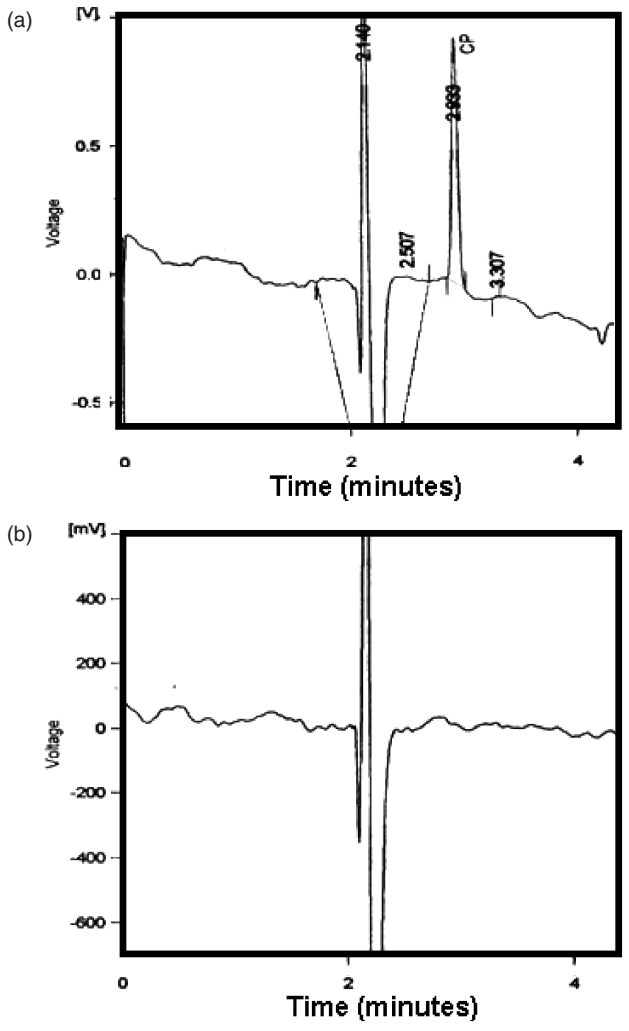


**Fig. 9.** Figure (A) shows the gas chromatogram of 1 l of the 50 ppb chlorpyrifos solution extracted with 150 ml of hexane thrice, evaporated to nearly 2 ml in rotavapor and made upto 10 ml using hexane. The peak at 2.933 is that of chlorpyrifos (labeled CP) and that at 2.14 is that of the solvent, B is the chromatogram of the chlorpyrifos solution (same concentration as above) after passing through the activated alumina column loaded with silver nanoparticles, extracted with hexane and made upto 10 ml as above, showing the complete disappearance of chlorpyrifos.

monitored by UV-Visible spectroscopy and the adsorption of pesticides on nanoparticles was confirmed by infrared spectroscopy. Complete removal of the pesticides from water was confirmed by UV-Visible spectroscopy and gas chromatography. The method offers a convenient and cost-effective means of removing pesticides from drinking water. Pure alumina alone is unable to remove the pesticides from water as shown by the control experiment. Experiments were conducted with an on-line water filter to demonstrate the use of this technology to rural communities.

**Acknowledgments:** The Nanoscience and Nanotechnology Initiative of the Department of Science and Technology, Government of India is thanked for equipment

RESEARCH ARTICLE

support. Eureka Forbes Limited, Bangalore is thanked for a few collaborative experiments and assistance with gas chromatography measurements.

## References and Notes


1. CEN (Chemical and Engineering News), Facts and Figures for Chemical Industry **(1997)**, Vol. 75, p. 25.
2. R. H. Plumb Jr., Ground Water Monitoring and Remediation **(1991)**, p. 157
3. S. C. Petrosius, R. S. Drago, V. Young, and G. C. Grunewald, *J. Am. Chem. Soc.* 115, 6131 **(1993)**.
4. J. Burns, and F. Miller, *Arch. Environ. Health* 30, 44 **(1975)**.
5. P. Schwarzebach and E. Molnar-Kubica, *Environ. Sci. Technol.* 13, 1367 **(1979)**.
6. B. Oliver, M. Charlton, and R. Durham, *Environ. Sci. Technol.* 23, 200 **(1989)**.
7. B. Oliver and K. Nicol, *Environ. Sci. Technol.* 16, 532 **(1982)**.
8. W.-X. Zhang, *J. Nanopart. Res.* 5, 323 **(2003)**.
9. C.-B. Wang and W.-X. Zhang, *Environ. Sci. Technol.* 31, 2154 **(1997)**.
10. W.-X. Zhang, C.-B. Wang, and H.-L. Lien, *Cat. Today* 40, 387 **(1998)**.
11. P. G. Tratnyek, *Chem. Indust.* 13, 499 **(1996)**.
12. N. Ichinose, Superfine Particle Technology, Springer, Berlin **(1992)**.
13. D. M. Cox, R. O. Brickman, K. Creegan, A. Kaldor, D L, Clusters and Cluster-Assembled Materials, edited by R. S. Nelson, Materials Research Society **(1991)**, p. 43.
14. A. S. Nair and T. Pradeep, *Curr. Sci.* 84, 1560 **(2003)**.
15. A. S. Nair, R. T. Tom, V. Suryanarayanan, and T. Pradeep, *J. Mater. Chem.* 13, 297 **(2003)**.
16. B. L. Brenner, S. Markowitz, M. Rivera, H. Romero, M. Weeks, E. Sanchez, E. Deych, A. Garg, J. Godbold, M. S. Wolff, P. J. Landrigan, and G. Berkowitz, *Environ. Health Persp.* 113, 1649 **(2003)**.
17. K. D. Racke, R. N. Lubinski, D. D. Fontaine, J. R. Miller, P. J. Mccall, and G. R. Oliver, *Acs. Sym. Ser.* 522, 70 **(1993)**.
18. S. M. Dyer, M. Cattani, D. L. Pisaniello, F. M. Williams, and J. Edwards, *Toxicology* 169, 177 **(2001)**.
19. D. J. Clegg and M. van Gemert, *J. Toxicol. Env. Heal. B* 2, 211 **(1999)**.
20. B. Luebke and B. Hum, *Ecol. Risk Assess.* 8, 293 **(2002)**.
21. J. L. Adgate, D. B. Barr, C. A. Clayton, L. E. Eberly, N. C. G. Freeman, P. J. Lioy, L. L. Needham, E. D. Pellizzari, J. J. Quackenboss, A. Roy, and K. Sexton, *Environ. Health Persp.* 109, 583 **(2001)**.
22. D. Zeljezic and V. Garaj-Vrhovac, *Chemosphere* 46, 295 **(2002)**.
23. J. Blasiak, P. Jaloszynski, A. Trzeciak, and K. Szyfter, *Mutat. Res-Gen Tox. En.* 445, 275 **(1999)**.
24. J. M. Pluth, J. P. O'Neill, J. A. Nicklas, and R. J. Albertini, *Mutat. Res.-Fund Mol.* 397, 137 **(1998)**.
25. J. M. Pluth, J. A. Nicklas, J. P. ONeill, and R. J. Albertini, *Cancer Res.* 56, 2393 **(1996)**.
26. P. Flessel, P. J. E. Quintana, and K. Hooper, *Environ. Mol. Mutagen* 22, 7 **(1993)**.
27. T. Galloway and R. Handy, *Ecotoxicology* 12, 345 **(2003)**.
28. T. Vial, B. Nicolas, and J. Descotes, *J. Toxicol. Env. Health* 48, 21 **(1996)**.
29. A. S. Nair, R. T. Tom, and T. Pradeep, *J. Environ. Monit.* 5, 363 **(2003)**.
30. B. V. Enustun and J. Turkevich, *J. A. Chem, Soc.* 85, 3317 **(1963)**.
31. P. V. Kamat, M. Flumiani, and G. V. Hartland, *J. Phys. Chem. B* 102, 3123 **(1998)**.
32. F. X. Zhong, L. Han, L. B. Israel, J. G. Daras, M. M. Maye, N. K. Ly, and C. J. Zhang, *Analyst* 127, 462 **(2002)**.
33. S. Link and M. A. El-Sayed, *Int. Rev. Phys. Chem.* 19, 409 **(2000)**.
34. M. M. Galera, J. L. M. Vidal, A. G. Frenich, and P. Parrilla, *Analyst* 119, 1189 **(1994)**.
35. G. Quintás, S. Garrigues, and M. de la Guardia, *Talanta* 63, 345 **(2003)**.
36. http://webbook.nist.gov/cgi/cbook.cgi?ID=C2921882&Units=SI&Mask=80.


Received: 16 March 2006. Accepted: 13 July 2006.